Zou et al. Journal of Translational Medicine (2025) 23:310
https://doi.org/10.1186/s12967-025-06320-w

Journal of Translational Medicine

RESEARCH Open Access

Single-cell analysis identifies MKI67$^+$ microglia as drivers of neovascularization in proliferative diabetic retinopathy

Keyi Zou[1†], Xue Li[1†], Bibo Ren[3], Fu Cheng[4], Jian Ye[1*] and Zelin Ou[2*]

Abstract

Background Proliferative diabetic retinopathy (PDR) is among the primary causes of blindness in individuals with diabetes. Elevated lactate levels have been identified as a critical biomarker associated with the prognosis of PDR. While significant lactate accumulation has been observed in the vitreous fluid of PDR patients, the detailed pathways through which lactate impacts pathological neovascularization remain insufficiently elucidated.

Methods The study employed single-cell RNA sequencing (scRNA-seq) to identify and characterize lactate-associated cell type in PDR patients. Key gene expression profiles and molecular pathways associated with lactate metabolism were analyzed. In vitro experiments were conducted using microglial cell cultures treated with high-glucose conditions (50 mM) to assess the induction of lactate metabolism-related genes. Additionally, an oxygen-induced retinopathy (OIR) mouse model was used to evaluate the impact of abemaciclib, an FDA-approved proliferation inhibitor, on retinal neovascularization.

Results To the best of our knowledge, this investigation is the first to delineate a novel microglial subset, designated as MKI67$^+$ microglia, distinguished by robust upregulation of genes implicated in lactate metabolic processes and proliferation, such as MKI67, PARK7 and LDHA, as well as a pronounced enrichment of glycolysis-associated molecular pathways. This unique cell type promotes angiogenesis by interacting with endothelial cells via secreted phosphoprotein 1 (SPP1)-Integrin alpha 4 (ITGA4) signaling. In vitro experiments have shown the use of 50 mM high glucose to simulate microglia in PDR environment and observe its promotion of vascular proliferation. In the in vivo OIR model, treatment with abemaciclib, a FDA-approved proliferation inhibitor, significantly reduced neovascularization.

Conclusion The identification of MKI67$^+$ microglia as a cell type strongly associated with lactate metabolism provides a novel perspective on the mechanisms underlying PDR onset. These findings expand our understanding of the cellular and metabolic dynamics in PDR, emphasizing potential implications for targeted therapeutic interventions.

Keywords Single cell analysis, Lactate metabolic gene, Proliferative diabetic retinopathy, Microglia, Abemaciclib, Oxygen-induced retinopathy

†Keyi Zou and Xue Li have contributed equally to this work.

*Correspondence:
Jian Ye
yejian1979@tmmu.edu.cn
Zelin Ou
13538697254@163.com
Full list of author information is available at the end of the article

Introduction

As the prevalence of diabetes continues to increase worldwide, diabetic retinopathy (DR) has emerged as a major cause of adult blindness, representing a substantial public health challenge due to its widespread occurrence and severe complications. [1–3] Among patients with a 10 year diabetes history, DR results in blindness for approximately 50%, and for those with over 15 years, the risk increases to nearly 80%. [4, 5] In its advanced stages, DR can progress to proliferative diabetic retinopathy (PDR), a severe form characterized by pathological neovascularization, leading to retinal hemorrhage, exudation, and edema, which severely impact vision [6, 7]. As PDR advances, fibrovascular proliferation may cause retinal traction, ultimately leading to detachment-a primary cause of irreversible vision loss. [8]

Lactate, a central product of glycolysis, plays a key role in cellular signaling and gene regulation under normal physiological conditions by balancing production and clearance [9–12]. In pathologic conditions such as hypoxia, oxidative phosphorylation in retinal cells is suppressed, leading to lactate buildup, which can alter protein function through lactic acid modification. [13, 14] For instance, hypoxia-driven lactic acid modification of the transcription factor YY1 (at K183) in microglia promotes FGF2 expression, thereby driving hypoxia-induced retinal neovascularization [15]. In diabetes, impaired glucose metabolism exacerbates lactate accumulation in the retina, disrupting cellular homeostasis and fostering an environment conducive to neovascularization [16]. Despite its recognized role, the specific mechanisms by which lactate regulates PDR progression remain largely unexplored.

Here, we used single-cell RNA sequencing data from the GEO database to map lactate metabolism-related genes (LMGs) expression in retinal cells from PDR patients. Our analysis identified a unique microglial subtype-MKI67$^+$ microglia (MKI67$^+$ MG)-characterized by high expression of lactate metabolism-associated and proliferation genes, and enrichment in glycolysis-related pathways. Under hyperglycemic conditions, these MKI67$^+$ MG promote endothelial cell proliferation and migration through SPP1/ITGA4, implicating them as key drivers of PDR pathogenesis. To explore therapeutic applications, we targeted MKI67$^+$ MG in an oxygen-induced retinopathy (OIR) mouse model with the FDA-approved proliferation inhibitor abemaciclib (Scheme 1). Treatment led to a significant reduction in MKI67$^+$ MG, accompanied by decreased neovascularization and vascular leakage. These findings provide novel insights into lactate's role and regulatory genes in PDR, establishing a cellular framework and initial evidence of abemaciclib's therapeutic potential.

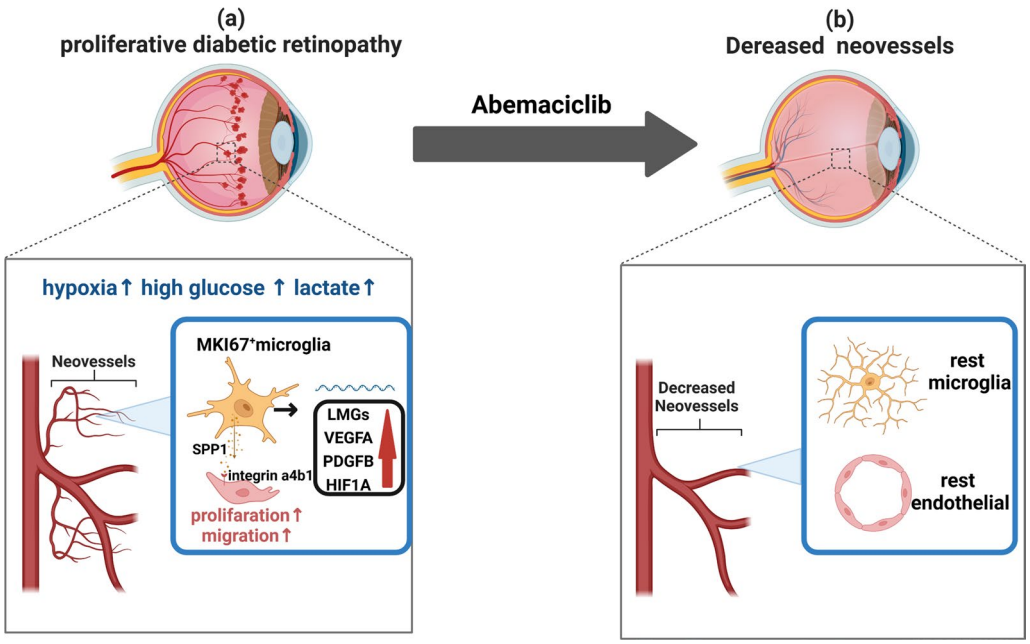

Scheme 1 **a** Mechanism of neovascularization driven by MKI67$^+$microglia in proliferative diabetes retinopathy. **b** FDA-approved proliferation inhibitor abemaciclib to suppress the positivity rate of MKI67$^+$ microglia, effectively reducing neovascularization

Materials and methods

Data sources

Gene expression matrix data (GSE165784) were obtained from the GEO database (http://www.ncbi.nlm.nih.gov/geo) for further analysis [18]. The dataset included five fibrovascular membrane (FVM) samples derived from patients diagnosed with proliferative diabetic retinopathy (PDR). Stringent quality control measures were applied to exclude low-quality cells, defined as those with unique molecular identifier (UMI) counts below 200 or above 3000, as well as cells exhibiting mitochondrial gene expression greater than 10%. Lactate metabolism-related gene sets were sourced from the Molecular Signatures Database (MSigDB; https://www.gsea-msigdb.org/gsea/msigdb/index.jsp). Using "lactate" as the query term, 12 high-priority lactate metabolism gene (LMG) sets were selected, including: (i) GOBP_lactate_metabolic_process, (ii) GOBP_lactate_transmembrane_transport, (iii) HP_abnormal_brain_lactate_level_by_mrs, (iv) HP_increased_circulating_lactate_concentration, (v) HP_increased_circulating_lactate_dehydrogenase_concentration, (vi) HP_abnormal_circulating_lactate_dehydrogenase_concentration, (vii) HP_abnormal_csf_lactate_concentration, (viii) HP_elevated_lactate_pyruvate_ratio, (ix) GOMF_lactate_dehydrogenase_activity, (x) GOMF_L_lactate_dehydrogenase_activity,(xi)GOMF_lactate_transmembrane_transport_activity, and (xii) WP_lactate_shuttle_in_glial_cells. Following the removal of redundant entries, a comprehensive set of 355 unique LMGs was finalized for subsequent analyses.

Analysis of single-cell transcriptomic data

Data analysis was conducted using the Seurat package to perform dimensionality reduction, clustering, and evaluation of the top 2000 highly variable genes. To ensure robust data quality, over 40,000 genes were retained for analysis. The "harmony" R package was employed to mitigate potential batch effects across samples, while data normalization was carried out using the ScaleData function. Cell-similarity relationships were established through the "FindNeighbors" function in Seurat, leveraging principal component analysis (PCA) dimensions. For refined clustering, the resolution parameter was set to 0.6. Visualization of clusters was achieved using uniform manifold approximation and projection (UMAP). Identification of cell clusters was guided by the expression profiles of well-established marker genes. Ultimately, cell types were annotated based on marker gene expression patterns within distinct clusters.

Cell function analysis

Gene Ontology (GO) and Kyoto Encyclopedia of Genes and Genomes (KEGG) pathway enrichment analyses were executed using the clusterProfiler4 package, which integrates comprehensive genome-wide annotation datasets curated by the Bioconductor project. Gene signature scores were calculated by the Seurat "AddModuleScore" function. CellPhoneDB was utilized to estimate cell–cell interactions. Cell lineage trajectories were inferred using "Monocle2" (version 2.10.0), thus facilitating the identification of cell transitions. Additionally, genes displaying significant changes over the pseudotime were identified.

Constructing an OIR mouse model

C57BL/6 J mice were obtained from the Laboratory Animal Center of the Army Medical University, China, and utilized to generate the oxygen-induced retinopathy (OIR) model. To induce retinal neovascularization, neonatal mice and their nursing mothers were subjected to hyperoxic conditions (75% oxygen) from postnatal day (P) 7 to P12, followed by a return to normoxic room air (21% oxygen). From P12 to P17, the pups were allocated into two groups: (i) intraperitoneal administration of abemaciclib (50 mg/kg) or (ii) vehicle control using the same solvent. On P17, mice were euthanized, and their eyes were harvested for subsequent analyses. Pups with body weights below 5 g on P17 were excluded from the study.

Quantitative real-time reverse transcription-polymerase chain reaction

Total RNA was isolated from retinal tissue or cell samples following the manufacturer's protocol for the Trizol reagent (Beyotime, R0016). The synthesis of complementary DNA (cDNA) was achieved using the First-Strand Synthesis System. Quantitative real-time reverse transcription PCR (qRT-PCR) analysis employed the TB Green® Premix Ex Taq™II reagent (TaKaRa, RR047A) on the StepOne Plus Real-Time PCR System. Gene-specific primers (Supplementary Table 1) were used to quantify mRNA levels. For normalization of expression, β-actin was used as the internal reference gene. Expression levels were calculated by the 2-ΔΔCT method, with results expressed as fold changes relative to controls.

Immunofluorescence staining

Mouse retinas were meticulously dissected from the eyes and incubated with primary antibodies. After thorough washing steps, the retinas were flat-mounted for additional processing. Primary antibodies included anti-IBA1 (diluted 1:100, Cell Signaling Technology, Cat# 17,198, RRID: AB_2820254) and anti-KI67 (diluted 1:100, Abcam, Cat# ab16667, RRID: AB_302459), along with

Isolectin GS-IB4 Alexa Fluor™ 568 (diluted 1:150–1:200, Molecular Probes, Cat# L21411, RRID: AB_2314665). Secondary antibodies conjugated to Alexa Fluor 488, 596, or 647 goat anti-rabbit IgG were then applied (diluted 1:400, Abcam, Cat# ab150077, RRID: AB_2630356; Abcam, Cat# ab150115, RRID: AB_2687948). Retinal whole mounts were finalized using an anti-fade medium containing DAPI for 30 min. Fluorescence imaging followed, and the resulting images were quantitatively analyzed using ImageJ software (National Institutes of Health, USA).

Co-culture of retinal microglial cells and human umbilical vein endothelial cells

Human microglial cells (HMCs, ATCC, Cat# CRL-3304, RRID: CVCL_II76) were obtained from Cell Biologics and maintained in accordance with the supplier's instructions. Human umbilical vein endothelial cells (HUVECs, ATCC, Cat# CRL-1730, RRID: CVCL_2959), sourced from the American Type Culture Collection (ATCC), were cultured in Dulbecco's Modified Eagle Medium (DMEM) supplemented with 10% fetal bovine serum and 1% penicillin–streptomycin. These cells were kept at 37 °C under a 5% CO_2 environment. HMCs and HUVECs in optimal growth conditions were plated in 12-well plates. For the co-culture experiments, HMCs were either preconditioned in high-glucose medium (50 mM) or cultured under normal glucose conditions for 24 h [17]. The supernatant from the HMC cultures was then transferred to the HUVEC wells for a 24 h co-culture. Afterward, HUVECs were separated, cultured in fresh medium for an additional 24 h, and subsequently harvested for further analysis.

Cell proliferation assay

To evaluate cell proliferation, human microglial cells (HMCs) pretreated with or without high glucose (50 mM) were co-cultured with Human umbilical vein endothelial cells (HUVECs) for 24 h. HUVECs were seeded into 96-well plates at a density of 1×10^4 cells per well for analysis. Proliferation was assessed using 5-ethynyl-2'-deoxyuridine (EdU) labeling, which was added to the culture medium at a final concentration of 10 μM for a 2 h incubation. Following incubation, cells were fixed with 4% paraformaldehyde for 15 min, then washed three times with phosphate-buffered saline (PBS). To permeabilize the cells, 0.1% Triton X-100 was applied on ice. EdU incorporation was detected using BeyoClick™ EdU-488 (Beyotime, C0071S) at room temperature in a light-protected environment. Hoechst 33,342 was subsequently added to stain nuclei under dark conditions. Fluorescence signals were captured and analyzed using confocal laser microscopy.

Wound healing assay

Initially, human umbilical vein endothelial cells (HUVECs) co-cultured with human microglial cells (HMCs) were either exposed to a high glucose concentration (50 mM) or maintained in standard conditions for 24 h. These cells were seeded onto 6-well plates and cultured overnight to reach 80% to 90% confluency. To simulate a wound gap, a marker was used to delineate the area along the back of the culture plates, followed by creating a straight scratch across the cell monolayer with a 10 μL pipette tip. Cells were then gently rinsed with PBS to clear debris, and 2 mL of serum-free DMEM was added per well. Cell migration was tracked by imaging at 0, 6, 12, and 24 h, with migration rates quantified using ImageJ software for accurate analysis.

Statistical analysis

All statistical analyses were performed with GraphPad Prism (GraphPad Software, CA). Independent-sample t-tests were utilized to compare qRT-PCR, cell proliferation assay, wound healing assay and neovascularization area data across groups. A P-value below 0.05 was regarded as statistically significant.

Results

scRNA-seq data integration and clustering of fibrovascular membrane

Figure 1 illustrates the flowchart of this study. First, single-cell RNA sequencing data from fibrovascular membrane of five samples diagnosed as PDR were integrated. After stringent quality control and filtering, 7764 cells were extracted for further analysis. Second, clustering was conducted using the UMAP method based on the GEO datasets, which yielded 16 original clusters (Fig. S1). Third, differentially expressed genes (DEGs) along with previously reported canonical markers annotated seven different cell types (Fig. 2a) and analyzed their proportions (Fig. 2b). Specifically, the characteristic gene markers of each cluster included the following: dendritic cells (markers: NAPSB, FCER1A, and CD1C), endothelial cells (markers: CLDN5, VWF, and SPARCL1), microglial cells (markers: CENPF, CX3CR1, SELENOP, HIST1H1B, GPNMB, FABP5, MRC1, and LIPA), fibroblasts (markers: COL1A1, AEBP1, THBS2, and CSPG4), pericytes (markers: ACTA2, PDGFRB, and RGS5), mono/macro (markers: LYZ, FCN1), and T cells (markers: TRBC2, LTB, and CD2) (Fig. S2). [18] Additionally, 355 LMGs were retrieved from the MSigDB database for subsequent bioinformatics analysis; they were defined as a gene set termed LMGs. Finally, cell-specific expression

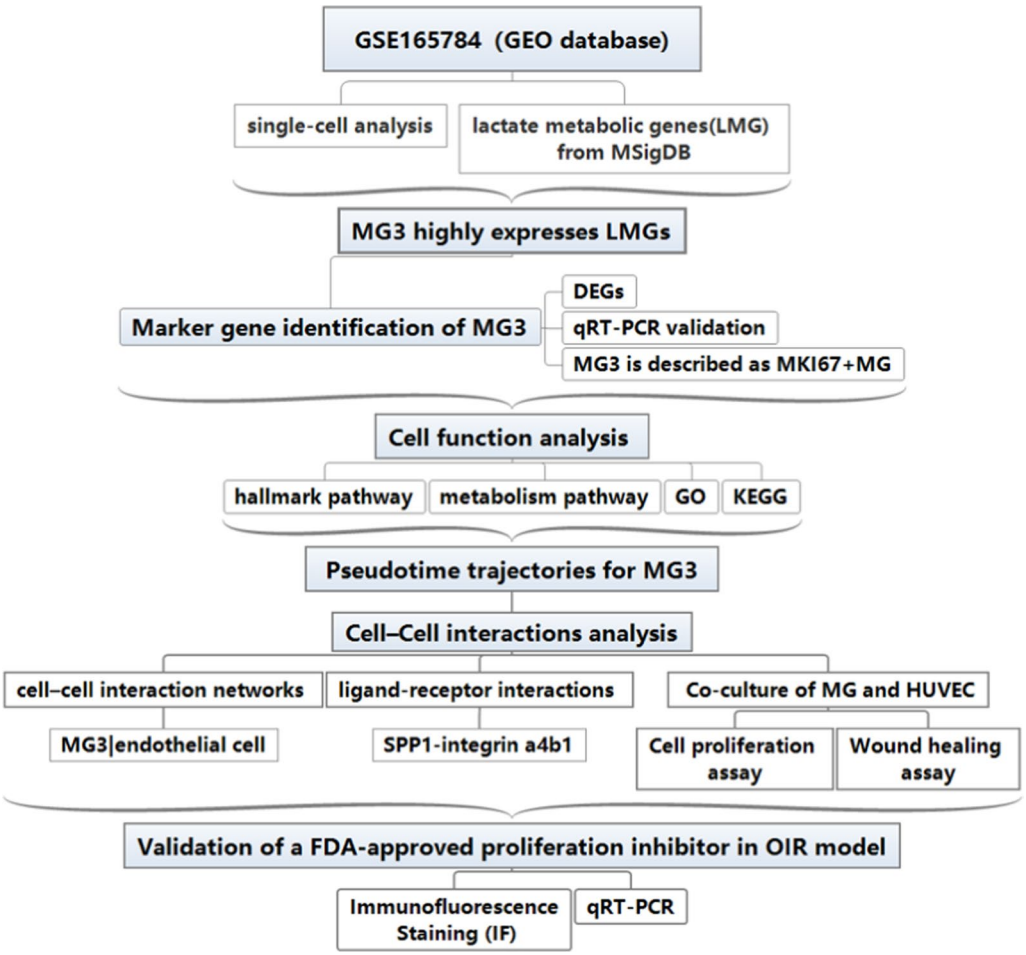

Fig. 1 Flow chart showing data collection and analysis

of this gene set was evaluated using cell scores, based on the average gene expression from the predefined gene set within respective cell types. The Seurat "Add Module Score" function was used in the default setting. The expression of LMGs was highest in the microglial cell subsets (Fig. 2c). Microglia are central to regulating retinal angiogenesis; they display widespread activation and accumulation around neovascular tufts in diabetic retinopathy [19, 20]. To investigate the distribution pattern of microglia, UMAP analysis was conducted to recluster these microglial cells into four subclusters, namely MG 0 to MG 3, according to similarities in gene expression (Fig. 2d). Additionally, each MG type was scored based on LMG expressions; the expression scores were significantly higher in the MG 3 subcluster, compared with the MG 0 to 2 subclusters (Fig. 2e). To establish the molecular differences among the four microglial clusters, their gene expression profiles were compared. The leading 5 DEG markers are shown in the heatmap; MG3 displayed the high MKI67 expression (Fig. 2f).

(See figure on next page.)

Fig. 2 scRNA-seq data integration and clustering **a** UMAP of key cell types in the GSE165784 dataset; the cells are color-coded by their sample identities. **b** Bar graph showing the percentage of each cluster from (**a**). Cell identity is determined based on the relative abundance of established markers. **c** LMG expression across different cell types in the fibrovascular membrane of patients with PDR. **d** UMAP plots of four clusters in microglial cells. **e** LMG expression score in microglial clusters MG 0 to MG 3. **f** Heatmap depicting the leading 5 signature gene expression profiles for the MG clusters. The upper bars denote the MG 0 to M3 groups. *UMAP* uniform manifold approximation and projection, *GSE* gene set enrichment, *LMG* lactate metabolism genes, *MG* microglia; and *PDR* proliferative diabetic retinopathy

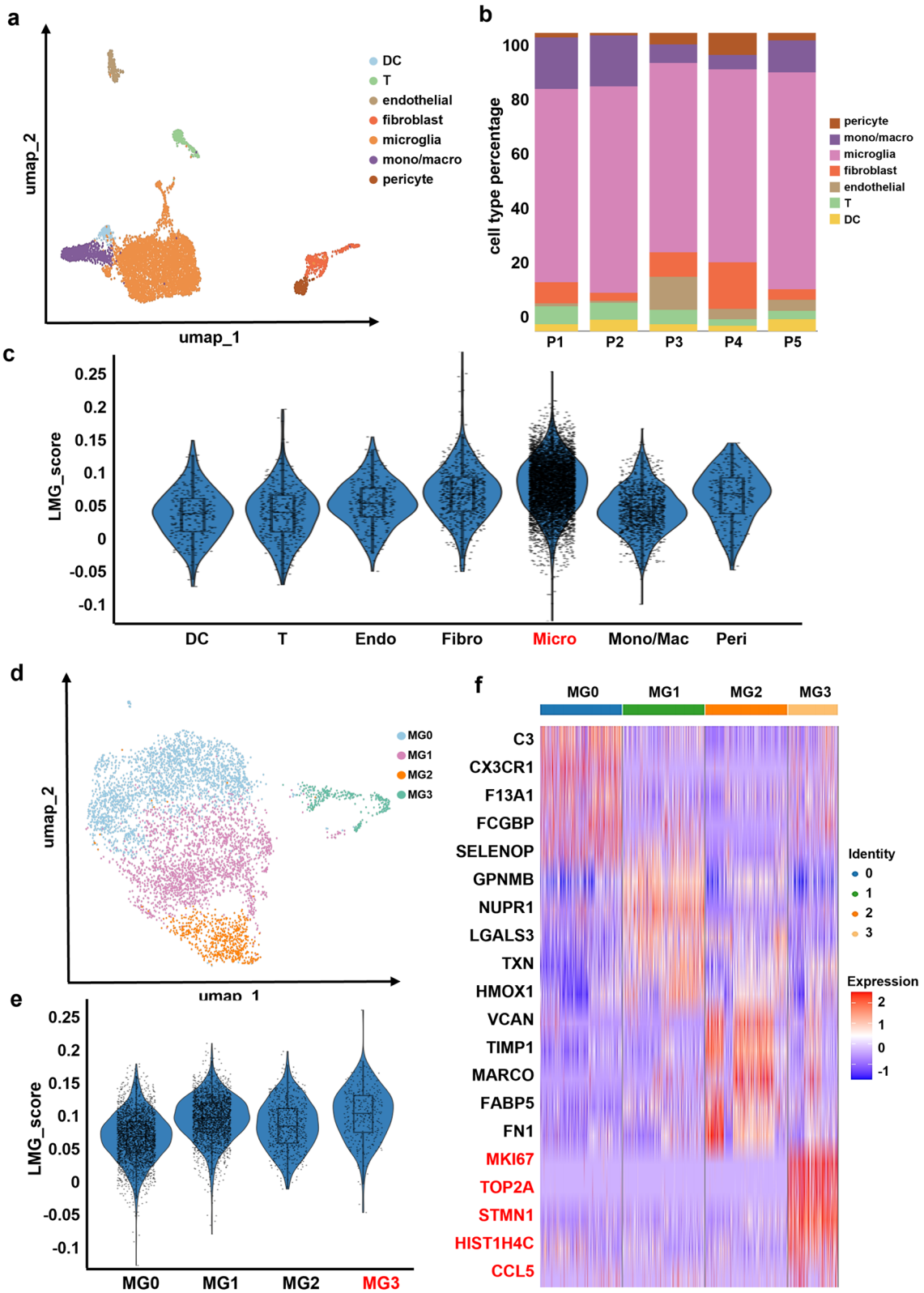

Fig. 2 (See legend on previous page.)

LMG expression profile analysis in microglial cells

The expression of LMGs was particularly elevated in MG 3. Thus, specific LMG expression profiles were identified in the highly proliferative microglial subpopulations. A differential expression analysis was conducted to compare MG 0, 1, 2, and 3, identifying 940 unregulated genes in MG 3 (Fig. 3a). This gene list was intersected with the predefined LMGs, and 38 overlapping genes were identified. This analysis generated proliferation-related genes along with six chief LMGs, namely secreted phosphoprotein 1 (SPP1), mitochondrially encoded cytochrome c oxidase II (MT-CO2), triosephosphate isomerase 1 (TPI1), enolase 1 (ENO1), lactate dehydrogenase A (LDHA), lactate dehydrogenase B (LDHB), and Parkinsonism-associated deglycase (PARK7) (Fig. 3b). UMAP plots demonstrated significant heterogeneity in the expression levels of the six LMGs across the four MG clusters. Notably, MG 3 expressed the highest expression levels than MG 0, 1, and 2 (Fig. 3c). Similarly, violin plots suggested an increased expression of the six LMGs, which corresponded with a transition from resting MG 0, 1, and 2 to the most proliferative MG 3 (Fig. 3d). Subsequently, this increased expression was affirmed through quantitative PCR of HMCs treated with high glucose (50 mM) or untreated controls (Fig. 3e, adj. p = 3.2e−14, 5.58e−12, 1.39e−8, 5.26e−7, 1.63e−7, 2.15e−8 respectively), consistent with the sc-RNA seq data results.

Functional analyses of the highly proliferative MG subpopulation

To explore the functional roles of MG 3, functional analyses were conducted using the genes unregulated in MG 3, compared with MG 0, 1, 2. Hallmark pathway analysis suggested that MG 3 demonstrated increased metabolism of pathways related to oxidative phosphorylation, mammalian target of rapamycin complex 1 signaling, glycolysis, and hypoxia (Fig. 4a), aligning with a hyper-lactate-metabolism phenotype in microglial subsets. Similarly, the metabolism pathway analysis indicated elevated pyruvate and propanoate metabolism (Fig. 4b). Consistent with this notion, GO analyses suggested significant involvement in processes, such as cellular respiration, oxidative phosphorylation, and active transmembrane transporter activity, suggesting the metabolic and energetic characteristics of MG 3. Furthermore, KEGG analyses confirmed that the DEGs in MG 3 were associated with cellular energy metabolism pathways (Fig. 4c). Analyzing the state trajectories and LMG trends in MG 3. To elucidate the gene expression dynamics within different microglial cells, pseudotemporal ordering was conducted across the four MG clusters (Fig. 4a). The split trajectories of each cell type demonstrated progression, initiating from MG 0, followed by MG 1 and MG 2, and finally MG 3. Figure 4b illustrates the state trajectories of the leading six upregulated genes in MG 3, particularly SPP1, MT-CO2, LDHA, LDHB, TPI1, and PARK7. Initially, these genes displayed a low expression, which increased progressively during pseudotime, aligning with previous findings about the highest LMG expressions in MG 3. Notably, the genes enriched for pyrimidine metabolism, glycolysis, base excision repair, HIF-1α signaling pathway, cell cycle, apoptosis, and pyruvate metabolism were significantly upregulated along the MG 3 trajectory (Fig. 4c).

Analyzing the state trajectories and LMG trends in MG 3

To elucidate the gene expression dynamics within different microglial cells, pseudotemporal ordering was conducted across the four MG clusters (Fig. 5a). The split trajectories of each cell type demonstrated progression, initiating from MG 0, followed by MG 1 and MG 2, and finally MG 3. Figure 5b illustrates the state trajectories of the leading six upregulated genes in MG 3, particularly SPP1, MT-CO2, LDHA, LDHB, TPI1, and PARK7. Initially, these genes displayed a low expression, which increased progressively during pseudotime, aligning with previous findings about the highest LMG expressions in MG 3. Notably, the genes enriched for pyrimidine metabolism, glycolysis, base excision repair, HIF-1 signaling pathway, cell cycle, apoptosis, and pyruvate metabolism were significantly upregulated along the MG 3 trajectory (Fig. 5c).

High-glucose-induced microglia regulates angiogenesis-related activities in HUVECs

To investigate the mechanism by which microglial cells promote angiogenesis, a heatmap depicting the interactions between endothelial cells and other cell types was generated (Fig. 6a). Notably, the interaction levels were high within MKI67$^+$ MG, indicating their involvement

(See figure on next page.)

Fig. 3 LMG expression analysis at single-cell level **a** Volcano plot displaying differentially expressed genes detected between MG 3 and MG 0, 1, and 2. **b** Intersection of upregulated genes between MG 3 and LMGs. **c** Representative gene expression profiles from the intersection gene set in MGs. **d** Violin plots of the differential expression for six key LMGs across the four clusters. **e** qPCR analysis of the representative LMG expressions in HMCs, either treated with high glucose or left untreated (n = 5). **p < 0.001 *LMG* lactate metabolism genes, *MG* microglia, and *qPCR* quantitative polymerase chain reaction

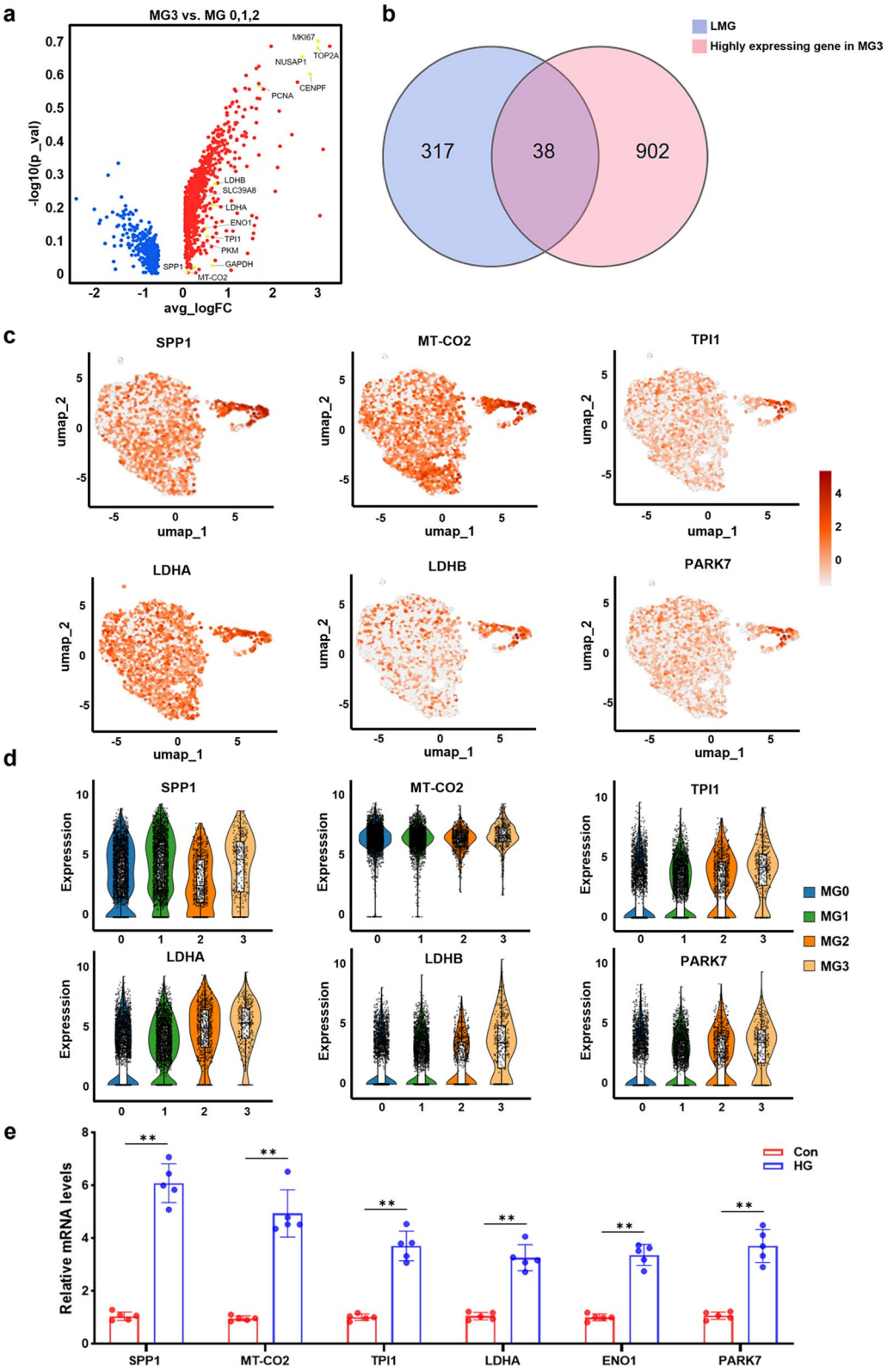

Fig. 3 (See legend on previous page.)

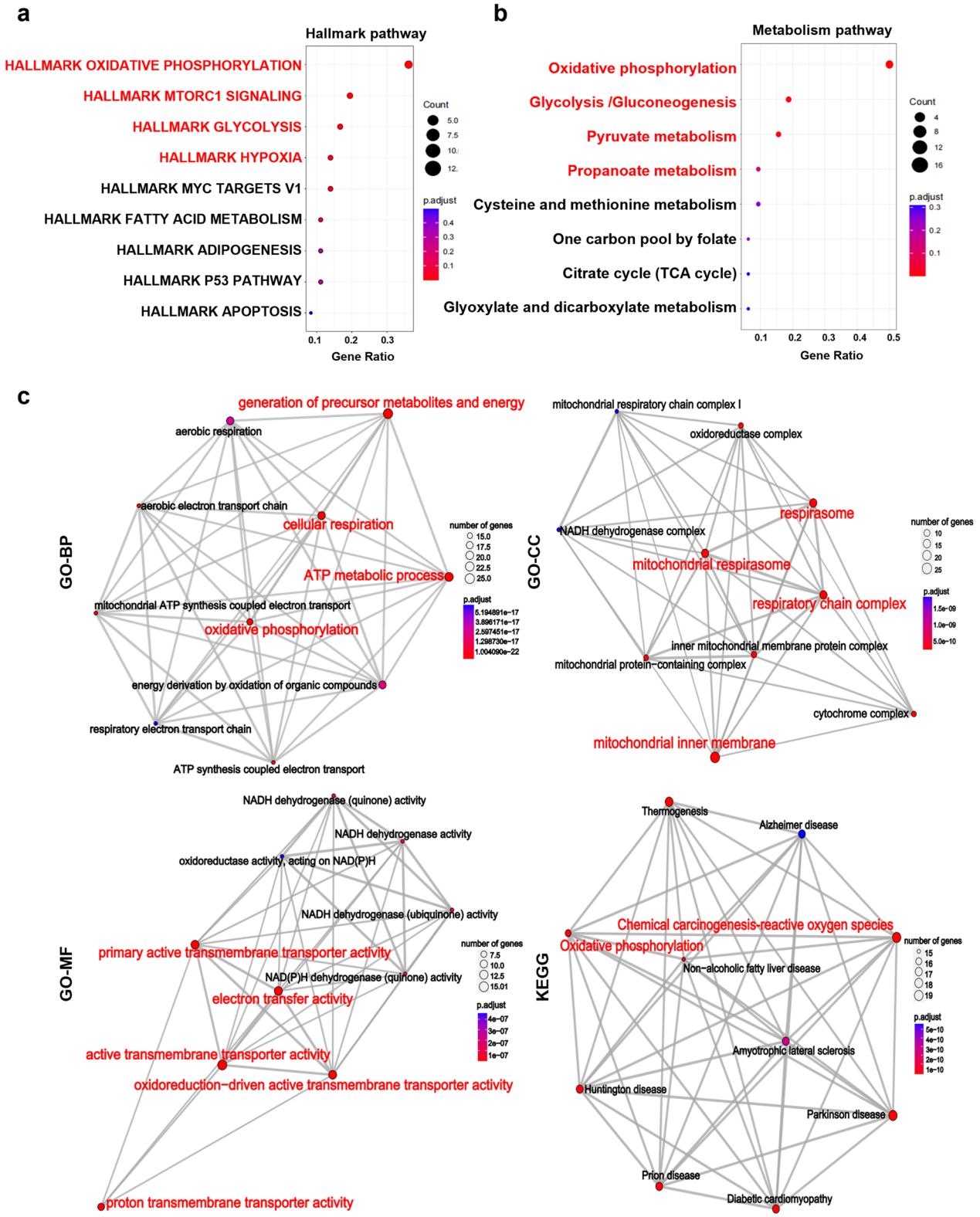

Fig. 4 Functional characterization of the identified microglial (MG) cluster. **a** Dot plot representing pathway enrichment analysis results from the Hallmark pathway database, highlighting relevant biological processes. **b** Dot plot depicting pathway enrichment derived from the Metabolism pathway database, underscoring metabolic alterations. **c** Emap plot illustrating integrated pathway enrichment findings across two independent pathway databases, utilizing lists of upregulated genes in MG 3 relative to MG 0, 1, and 2 for comparative analysis. *MG* microglia

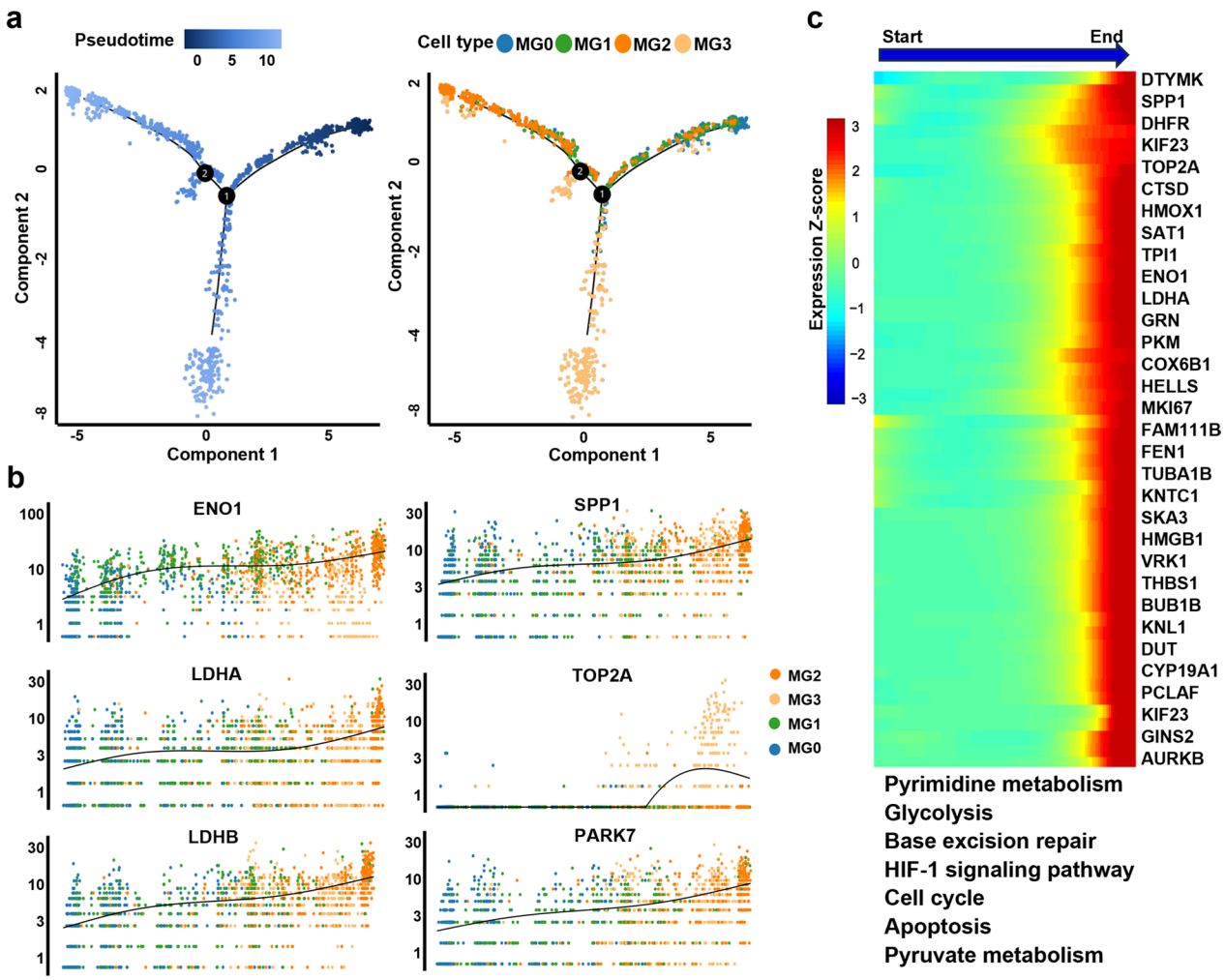

Fig. 5 State trajectories and expression trends of LMGs in MG 3 **a** Pseudotime trajectories for MG 3 showing branching patterns that differentiate into different cell subtypes. **b** Dynamic expression patterns of representative LMGs along the trajectory. **c** Heatmap showing upregulated genes and representative pathways enriched along the trajectory in MG 3. *LMG* lactate metabolism genes, *MG* microglia

in the biological behavior of endothelial cells. A cell–cell communication network was constructed based on the ligand-receptor pair expression profiles in each cell type (Fig. 6b). Furthermore, these cells exhibited upregulated SPP1 ligand expression and Integrin_a4b1_complex receptors (Fig. 6c). Correlation analysis revealed a positive relationship between lactate metabolism gene (LMG) scores and the expression of known proangiogenic

(See figure on next page.)

Fig. 6 Mechanism of microglia in PDR retinal microenvironment to regulate the angiogenesis-related activities of HUVECs **a** Heatmap of the interaction strength among MKI67$^+$MG and other cell types. The color showed the interaction strength that was calculated by cellchat. **b** Cell–cell interaction networks among 8 cell subtypes based on CellPhoneDB. **c** Bubble plots of molecular interaction states of 8 common ligand-receptor pairs (rows) between MKI67 + MG and other cell type. **d** The correlations between LMG score and the expression level of proangiogenic factors, *** $p < 0.001$. **e** Experimental workflow for co-culture of HMCs treated by high glucose and HUVEC. **e** Schemetic drawing of col-culture. **f** EdU incorporation assay results reveal the proliferative capacity of HUVECs across different treatment conditions. Values are shown as mean ± SD, with n = 5 per group. Three visual fields were selected from a single well per group to calculate the mean (one-way ANOVA). Scale bars represent 50 μm. **g** Wound healing assay results indicate the migration rates of HUVECs exposed to varying treatments. Results are displayed as mean ± SD, with n = 3 per group, averaging across three visual fields per well (one-way ANOVA). Scale bars correspond to 200 μm. Significance levels: * $p < 0.05$, ** $p < 0.001$. *LMG* lactate metabolism genes, *MG* microglia, *PDR* proliferative diabetic retinopathy, *HUVECs* human umbilical vein endothelial cells, *HMCs*, human microglial cells, *ANOVA* analysis of variance, *SPP1* secreted phosphoprotein 1, EdU, 5-ethynyl-2′-deoxyuridine. **h** qPCR analysis of SPP1 expression in HMCs, either treated with high glucose or left untreated (n=5)

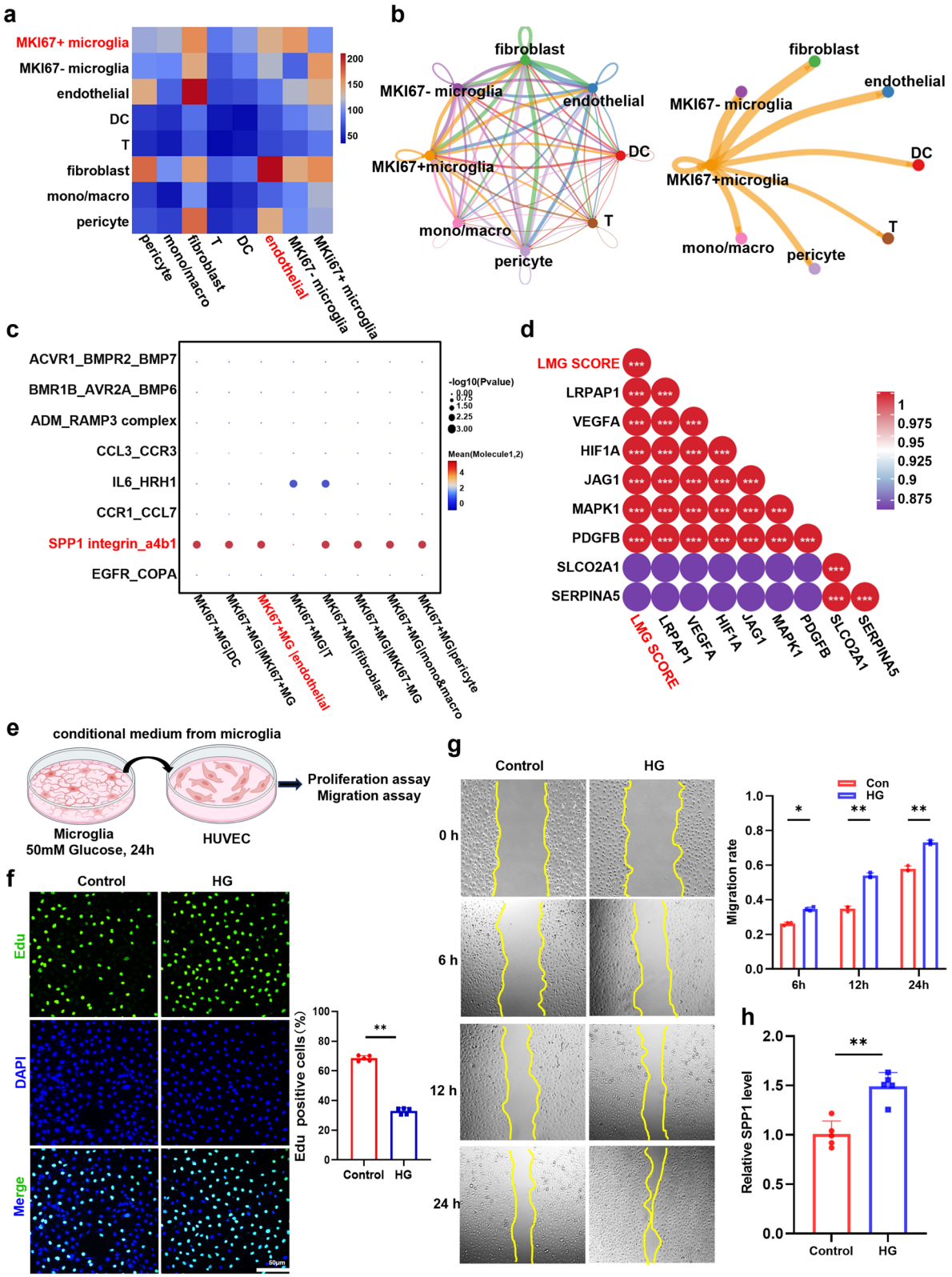

Fig. 6 (See legend on previous page.)

factors, including vascular endothelial growth factor A (VEGFA), HIF1A, and platelet-derived growth factor subunit B (PDGFB) (Fig. 6d) [23]. To investigate the role of microglia-endothelial cell interactions, HUVECs were cultured with either DMEM or conditioned medium (CM) derived from high glucose–treated HMCs (Fig. 6e). Compared with treatment with DMEM alone, exposure to CM significantly enhanced HUVEC proliferation and migration (Fig. 6f, g). Intriguingly, qPCR results suggested that high-glucose exposure significantly induced Spp1 levels in HMCs (Fig. 6h, p = 0.00054), confirming SPP1 as a high-glucose-inducible gene. SPP1 is central to retinal neovascularization. [21, 22] Our findings implicate SPP1 as a crucial component of angiogenic activity in retinal neovascularization.

Correlation analysis revealed a positive relationship between lactate metabolism gene (LMG) scores and the expression of known proangiogenic factors, including vascular endothelial growth factor A (VEGFA), HIF1A, and platelet-derived growth factor subunit B (PDGFB) (Fig. 6d) [23]. To investigate the role of microglia-endothelial cell interactions, HUVECs were cultured with either DMEM or conditioned medium (CM) derived from high-glucose-treated HMCs (Fig. 6e). Exposure to CM significantly enhanced HUVEC proliferation and migration compared to DMEM treatment alone (p = 2.29e−9 in Fig. 6f, adj. p = 0.0236, 0.0011, 0.0027 respectively in Fig. 6g). These findings collectively suggest that MKI67$^+$ MG facilitate endothelial cell proliferation and migration.

Effects of abemaciclib on retinal neovascularization in the OIR model

To explore the proangiogenic mechanisms underlying MKI67$^+$ microglia, the therapeutic efficacy of anti-proliferation therapy was assessed. To this end, abemaciclib, a FDA-approved proliferation inhibitor, [24, 25] was utilized in the OIR model. First, numerous cell types expressed KI67, with microglia cells displaying the highest expression (Fig. 7a), serving as the key target for abemaciclib. Second, after constructing the OIR model, neonatal mice were injected with either corn oil (control) or abemaciclib (50 mg/kg) intraperitoneally from P12 to P17. Subsequently, whole retina tissues were collected on P17 and analyzed (Fig. 7b). Expectedly, neonatal mice treated with abemaciclib demonstrated significantly reduced retinal neovascularization tufts, hemangioma, and vascular leakage, compared with the controls (Fig. 7c, p = 2.87e−8), indicating the therapeutic potential of Ki67 signaling blockage for retinal neovascular diseases. LMG genes, proangiogenic factors (Hif1a, Vegfa, Ldha, Pdgfb) and Ki67 gene levels were significantly lower in the retinas of the abemaciclib group than in the retinas of the control group (Fig. 7d, p = 6.35e−7, 1.89e−4, 5.92e−4, 4.91e−4 and 0.0011 respectively). Multiple immune fluorescence staining was conducted with the proliferation marker (Ki67) and the microglia marker (Iba1) in OIR retinas; it confirmed the presence of proliferative and active microglia adjacent to neovascularization tufts, as displayed by isolectin B4-induced colocalization [19]. In contrast, Ki67$^+$ MG was barely observed in abemaciclib-injected retinas, accompany with a significant decrease in retinal neovascularization (Fig. 7e). These findings provide novel insights into targeting highly proliferative microglia to alleviate angiogenesis in the ischemia/hypoxia-induced retinopathy.

Discussion

Lactic acid serves as a key mediator in transcriptional control, DNA repair, and the regulation of mitochondrial respiratory dynamics [26–28]. As a king of chronic diseases, lactic acid is often regarded as a prognostic biomarker of diabetes [29]. However, increased lactic acid levels have been observed in the vitreous humor in PDR cases, a complication that leads to blindness in patients with diabetes [30]. The mechanism by which lactic acid regulates neovascularization remains largely unexplored. In this study, single-cell RNA sequencing (scRNA-seq) data from the GEO database were utilized to investigate cellular heterogeneity within the fibrovascular proliferative membranes of PDR patients. The analysis focused on the expression profiles of lactate metabolism-related genes (LMGs) to identify critical cell types and their roles in the underlying pathological mechanisms. Notably, this is the first study to report the identification of

(See figure on next page.)

Fig. 7 Effects of abemaciclib on retinal neovascularization in the OIR model **a** MKI67 expression across cell types in the fibrovascular membrane in patients with PDR. **b** An experimental scheme shows the OIR mice model induced on P7. Abemaciclib (50 mg/kg) with or a similar amount of corn oil was intraperitoneally injected into the contralateral eye on P12; the mice were humanely killed on P17. **c** Immunofluorescence analysis of whole retinal flat-mounts from OIR P17 stained with IB4 (red), including quantification of neovascularized area percentages (mean ± SD; n = 5 per group; unpaired Student's t-test). Scale bar: 50 μm. **d** qPCR results showing expression levels of proangiogenic factors and ki67 (n = 3 per group), with significance levels *P < 0.05 and **P < 0.001. **e** Immunofluorescence imaging displays nuclear Ki67$^+$ cells (marked with green), microglia/macrophages labeled with Iba1 (white), and vasculature marked by isolectin B4 (red) in whole-mount retinas from both OIR and OIR + abemaciclib conditions (n = 3 per group). Scale bars: 50 μm and 20 μm (far-right panel). *LMG* lactate metabolism genes, *OIR* oxygen-induced retinopathy, *PDR* proliferative diabetic retinopathy

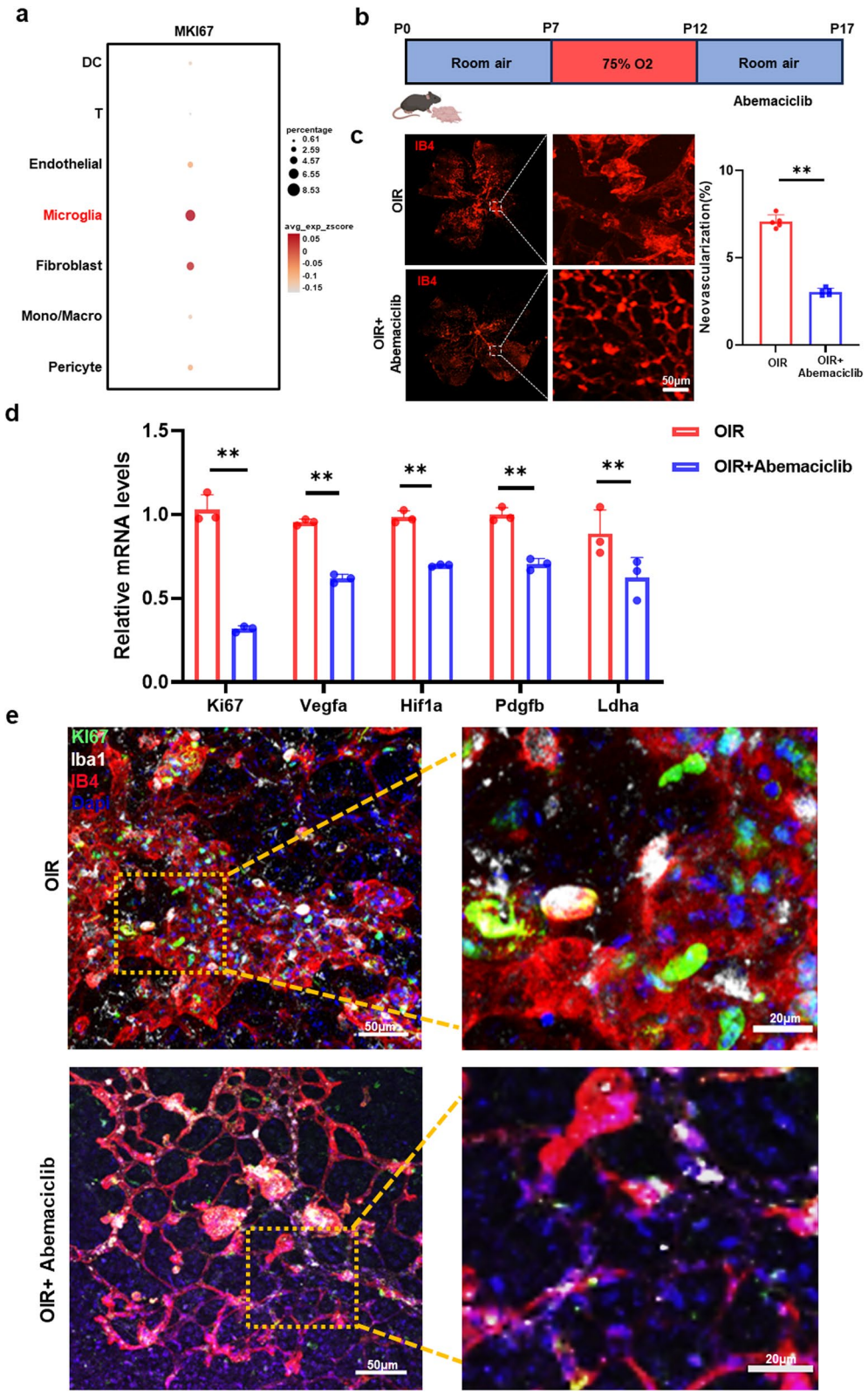

Fig. 7 (See legend on previous page.)

a microglial subpopulation, termed MKI67$^+$ MG, which exhibits high expression of the MKI67 gene and is strongly linked to lactate metabolism. The discovery of MKI67$^+$ MG offers a novel framework for understanding the pathogenesis of PDR and highlights potential targets for therapeutic intervention.

Similarly, other researchers analyzed single-cell retinal data using an OIR mouse model; they identified a highly proliferative microglial subpopulation, characterized by ki67 gene expression. These microglia were abundant around the clusters of pathological neovascularization [31]. Therefore, MKI67$^+$ microglia may be involved in excessive vascular growth of blood vessels in PDR. To investigate the mechanism by which MKI67$^+$ microglia promoting neovascularization, we conducted detailed HALLMARK, METABOLISM pathway, KEGG, and GO pathway analyses. MKI67$^+$ microglia demonstrated significant enrichment in critical metabolic pathways, such as oxidative phosphorylation, glycolysis/gluconeogenesis, and pathways associated with energy metabolism.

Subsequently, a pseudotemporal analysis was conducted to investigate whether LMGs affect the differentiation trajectory of MKI67$^+$ MG. Changes in the expression of these genes were strongly associated with the differentiation process of MKI67$^+$ MG. Therefore, lactate metabolism may serve as a key driving factor in MKI67$^+$ MG differentiation. This finding provides novel insights into the abnormal activation and differentiation of microglia in PDR. Additionally, the intercellular communication analysis suggested a complex network of interactions between MKI67$^+$ MG and other cell types. Specifically, MKI67$^+$ MG promote angiogenesis through the secretion of SPP1, which eventually acts on Integrin α4β1 receptors on endothelial cells. This mechanism of action explains the importance of the SPP1-Integrin α4β1 axis in PDR angiogenesis. Additionally, it elucidates the process by which lactate metabolism and its downstream effectors control the behavior of MKI67$^+$ MG during PDR angiogenesis.

To confirm these findings, in vitro, co-culture experiments were conducted by exposing microglia to high-glucose conditions to simulate the PDR microenvironment. This serves as the foundation for subsequent experiments. The supernatant from the culture medium comprising high-glucose-treated microglia was co-cultured with HUVECs. Moreover, the high-glucose-treated microglia demonstrated a significantly increased ability to release Spp1 level. Simultaneously, a characteristic increase in the migration and proliferation abilities of endothelial cells was observed. These results strongly support our hypothesis that MKI67$^+$ MG may promote endothelial cell activation and neovascularization through the secretion of factors, such as SPP1. Finally, to explore the effective therapeutic strategies targeting MKI67$^+$ MG in PDR, the OIR model was constructed. It closely mimics the microenvironment of PDR in vivo [32]. This model was used to assess the therapeutic efficacy of abemaciclib, a FDA-approved proliferation inhibitor. Treatment with abemaciclib significantly reduced retinal neovascularization. Notably, immunofluorescence analysis indicated that the number of Ki-67-positive microglia was significantly reduced in the abemaciclib-treated group as opposed to the control group, thereby underscoring the inhibitory impact of abemaciclib on microglial proliferation.

Previously, researchers confirmed the role of lactate and lactylation in ocular neovascularization [15]. To the best of our knowledge, this study represents the first comprehensive characterization of a distinct cell type intricately associated with lactate metabolism in the pathogenesis of PDR.

This study has some limitations. The findings demonstrated that inhibiting MKI67$^+$ MG significantly reduces retinal neovascularization; however, it remains unclear whether this MKI67$^+$ MG possesses other characteristics, such as regulating the PDR inflammatory microenvironment. Further research will help us understand the pathogenesis of PDR and provide a theoretical basis for designing more drugs targeted at MKI67$^+$ MG.

In summary, this study utilized scRNA-seq data from the fibrovascular membranes of patients with PDR. It identified a key subpopulation of cells, MKI67$^+$ MG, strongly associated with lactate metabolism. Additionally, it described their genetic markers, lactate metabolism-related gene expression, signaling pathways, and cell differentiation trajectories, explaining their role in promoting angiogenesis through metabolism- and immune-related mechanisms of action. Additionally, in vitro experiments and animal model validation helped us explore a novel treatment strategy for PDR and other microglia-regulated ocular neovascularization diseases by inhibiting their proliferation. In the future, researchers are required to focus on the origin, differentiation regulation, and inhibition of MKI67$^+$ MG to advance the treatment of PDR.

Supplementary Information

The online version contains supplementary material available at https://doi.org/10.1186/s12967-025-06320-w.

Supplementary Material 1.

Acknowledgements

This research was supported by grant 82171054 (to Y.J.) from the National Natural Science Foundation of China and grant CSTB2023NSCQ-MSX0593 (to L.X.) from Chongqing Natural Science Foundation.

Author contributions
Conceptualization: Zelin Ou and Jian Ye; data analysis: Keyi Zou, Xue Li and Bibo Ren; Data curation: Xue Li; Data interpretation and Investigation: Keyi Zou and Xue Li; Data visualization: Keyi Zou, Xue Li and Fu Cheng; Resources: Keyi Zou and Jian Ye; Funding acquisition: Jian Ye; Writing Original draft: Keyi Zou and Xue Li; Writing Review and editing: Zelin Ou, Jian Ye, Keyi Zou and Xue Li; Supervision: Zelin Ou, Jian Ye, Keyi Zou and Xue Li. All authors read, revised, and approved the final manuscript. Keyi Zou and Xue Li contributed equally.

Data availability
The data that support the findings of this study are available from the corresponding author upon reasonable request.

Declarations

Ethics approval and consent to participate
All procedures were approved by the Laboratory Animal Welfare and Ethics Committee of the Army Medical University, China (Approval No. AMU-WEC20247083) and conducted in compliance with the ARVO Statement for the Use of Animals in Ophthalmic and Vision Research.

Competing interests
The authors declare that they have no competing interests.

Author details
[1]Department of Ophthalmology, The Third Hospital Affiliated to the Third Military Medical University Department of Ophthalmology, Chongqing 400042, China. [2]Department of Dermatology, Children'S Hospital of Chongqing Medical University, Chongqing 400014, China. [3]College of Biomass Science and Engineering, Sichuan University, Chengdu 610065, China. [4]The Second School of Clinical Medicine, Southern Medical University, Guangzhou 510080, Guangdong, China.

Received: 25 November 2024 Accepted: 25 February 2025
Published online: 11 March 2025

References

1. Leasher JL, Bourne RRA, Flaxman SR, Jonas JB, Keeffe J, Naidoo K, et al. Global estimates on the number of people blind or visually impaired by diabetic retinopathy: a meta-analysis from 1990 to 2010. Diabetes Care. 2016;39(9):1643–9.
2. Lundeen EA, Burke-Conte Z, Rein DB, Wittenborn JS, Saaddine J, Lee AY, et al. Prevalence of diabetic retinopathy in the US in 2021. JAMA Ophthalmol. 2023;141(8):747–54.
3. Teo ZL, Tham Y-C, Yu M, Chee ML, Rim TH, Cheung N, et al. Global prevalence of diabetic retinopathy and projection of burden through 2045: systematic review and meta-analysis. Ophthalmology. 2021;128(11):1580–91.
4. Li X, Tan T-E, Wong TY, Sun X. Diabetic retinopathy in China: epidemiology, screening and treatment trends—a review. Clin Experiment Ophthalmol. 2023;51(6):607–26.
5. Solomon SD, Chew E, Duh EJ, Sobrin L, Sun JK, VanderBeek BL, et al. Diabetic retinopathy: a position statement by the American diabetes association. Diabetes Care. 2017;40(3):412–8.
6. Sun JK, Liu D. Challenges in the clinical management of proliferative diabetic retinopathy: treatment choice and follow-up. JAMA Ophthalmol. 2023;141(1):46–7.
7. Crabtree GS, Chang JS. Management of complications and vision loss from proliferative diabetic retinopathy. Curr DiabRep. 2021;21(9):33.
8. Tamaki K, Usui-Ouchi A, Murakami A, Ebihara N. Fibrocytes and fibrovascular membrane formation in proliferative diabetic retinopathy. Invest Ophthalmol Vis Sci. 2016;57(11):4999–5005.
9. Fang Y, Li Z, Yang L, Li W, Wang Y, Kong Z, et al. Emerging roles of lactate in acute and chronic inflammation. Cell Commun Signal. 2024;22(1):276.
10. Li X, Yang Y, Zhang B, Lin X, Fu X, An Y, et al. Lactate metabolism in human health and disease. Signal Transduct Target Ther. 2022;7(1):305.
11. Wang J, Wang Z, Wang Q, Li X, Guo Y. Ubiquitous protein lactylation in health and diseases. Cell Mol Biol Lett. 2024;29(1):23.
12. Zhang D, Tang Z, Huang H, Zhou G, Cui C, Weng Y, et al. Metabolic regulation of gene expression by histone lactylation. Nature. 2019;574(7779):575–80.
13. Lee D, Tomita Y, Miwa Y, Kunimi H, Nakai A, Shoda C, et al. Recent insights into roles of hypoxia-inducible factors in retinal diseases. Int J Mol Sci. 2024;25(18):10140.
14. Vohra R, Kolko M. Lactate: more than merely a metabolic waste product in the inner retina. Mol Neurobiol. 2020;57(4):2021–37.
15. Wang X, Fan W, Li N, Ma Y, Yao M, Wang G, et al. YY1 lactylation in microglia promotes angiogenesis through transcription activation-mediated upregulation of FGF2. Genome Biol. 2023;24(1):87.
16. Chen X, Wang Y, Wang J-N, Zhang Y-C, Zhang Y-R, Sun R-X, et al. Lactylation-driven FTO targets CDK2 to aggravate microvascular anomalies in diabetic retinopathy. EMBO Mol Med. 2024;16(2):294–318.
17. Huang Z, Liang J, Chen S, Ng TK, Brelén ME, Liu Q, et al. RIP3-mediated microglial necroptosis promotes neuroinflammation and neurodegeneration in the early stages of diabetic retinopathy. Cell Death Dis. 2023;14(3):227.
18. Hu Z, Mao X, Chen M, Wu X, Zhu T, Liu Y, et al. Single-cell transcriptomics reveals novel role of microglia in fibrovascular membrane of proliferative diabetic retinopathy. Diabetes. 2022;71(4):762–73.
19. Usui-Ouchi A, Usui Y, Kurihara T, Aguilar E, Dorrell MI, Ideguchi Y, et al. Retinal microglia are critical for subretinal neovascular formation. JCI Insight. 2020. https://doi.org/10.1172/jci.insight.137317.
20. Hu A, Schmidt MHH, Heinig N. Microglia in retinal angiogenesis and diabetic retinopathy. Angiogenesis. 2024;27(3):311–31.
21. Shi H, Yin Z, Koronyo Y, Fuchs D-T, Sheyn J, Davis MR, et al. Regulating microglial miR-155 transcriptional phenotype alleviates Alzheimer's-induced retinal vasculopathy by limiting Clec7a/Galectin-3+ neurodegenerative microglia. Acta Neuropathol Commun. 2022;10(1):136.
22. Wang T, Kaneko S, Kriukov E, Alvarez D, Lam E, Wang Y, et al. SOCS3 regulates pathological retinal angiogenesis through modulating SPP1 expression in microglia and macrophages. Mol Ther. 2024;32(5):1425–44.
23. Chen L, Zhang H, Zhang Y, Li X, Wang M, Shen Y, et al. Ganglion cell-derived LysoPS induces retinal neovascularisation by activating the microglial GPR34-PI3K-AKT-NINJ1 axis. J Neuroinflammation. 2024;21(1):278.
24. Kim ES. Abemaciclib: first global approval. Drugs. 2017;77(18):2063–70.
25. Stirrups R. Abemaciclib plus fulvestrant for breast cancer. Lancet Oncol. 2019;20(11): e617.
26. Cai X, Ng CP, Jones O, Fung TS, Ryu KW, Li D, et al. Lactate activates the mitochondrial electron transport chain independently of its metabolism. Mol Cell. 2023;83(21):3904–20.
27. Chen H, Li Y, Li H, Chen X, Fu H, Mao D, et al. NBS1 lactylation is required for efficient DNA repair and chemotherapy resistance. Nature. 2024;631(8021):663–9.
28. Chen Y, Wu J, Zhai L, Zhang T, Yin H, Gao H, et al. Metabolic regulation of homologous recombination repair by MRE11 lactylation. Cell. 2024;187(2):294-311.e21.
29. Wang X, Yang S, Yang G, Lin J, Zhao P, Ding J, et al. Novel risk score model for non-proliferative diabetic retinopathy based on untargeted metabolomics of venous blood. Front Endocrinol. 2023. https://doi.org/10.3389/fendo.2023.1180415.
30. Tomita Y, Cagnone G, Fu Z, Cakir B, Kotoda Y, Asakage M, et al. Vitreous metabolomics profiling of proliferative diabetic retinopathy. Diabetologia. 2021;64(1):70–82.
31. Liu Z, Shi H, Xu J, Yang Q, Ma Q, Mao X, et al. Single-cell transcriptome analyses reveal microglia types associated with proliferative retinopathy. JCI Insight. 2022. https://doi.org/10.1172/jci.insight.160940.
32. Liu Z, Yan S, Wang J, Xu Y, Wang Y, Zhang S, et al. Endothelial adenosine A2a receptor-mediated glycolysis is essential for pathological retinal angiogenesis. Nat Commun. 2017;8(1):584.

Publisher's Note